Production and Characterization of Polycaprolactone Nanofibers via Forcespinning™ Technology

Zachary McEachin, Karen Lozano

Department of Mechanical Engineering, University of Texas-Pan American, Edinburg, Texas 78539

Received 31 May 2011; accepted 18 December 2011
DOI 10.1002/app.36843
Published online in Wiley Online Library (wileyonlinelibrary.com).

ABSTRACT: Among the myriad of methods for polymer nanofiber production, there are only a few methods that can produce submicron range fibers in bulk from melt or solution samples. The Forcespinning™ method allows a substantial increase in sample yield while simultaneously maintaining the integrity of uniform fibers in the nanometer range. The high production yield of such a method greatly reduces the time needed to produce bulk quantities of fibers which may be critical in many fields of research and industry, in particularly in fields relating to biopolymers. The aim of this study was to use this method to form nonwoven mats of polycaprolactone (PCL) nanofibers and to quantitatively analyze the production and characterization of the produced fibers. The bulk PCL was dissolved in dichloromethane and the solutions were forcespun at varying speeds ranging from 3000 to 9000 rpm. It was observed that fiber diameter decreased with increasing rotational speed. The average fiber diameter at 9000 rpm was 220 nm with a standard deviation of ±98 nm. The morphology and degree of crystallinity were characterized by scanning electron microscopy, differential scanning calorimetry, and X-ray diffraction. © 2012 Wiley Periodicals, Inc. J Appl Polym Sci 000: 000–000, 2012

Key words: biopolymers; differential scanning calorimetry; electron microscopy

INTRODUCTION

The production of fine polymer fibers has recently garnered much attention due to their potential applications. These nanofibrous polymers are unique due in part to their superior mechanical properties, large surface area to volume ratio, and their potential to resemble cellular topographies. Nonwoven polymer fibers in the nanometer range are currently being investigated for uses in filtration, composite reinforcements, chemical sensors, and tissue scaffolding.[1–4] Despite the recent interest in nonwoven nanofibers, significant challenges remain in their implementation due to the lack of high throughput production.

In the last few decades, electrospinning has been the most widely used[5,6] and promising method of producing fine fibers.[7] Electrospinning uses high-voltage electrostatic forces between an electrically charged polymer solution fed via a metering pump and a conductive collector to initiate fiber formation.[8] Although a simple and laboratory efficient method for fiber production, the electrospinning method poses many disadvantages including: (1) use of a high-voltage power source (>10 kV), (2) limited to solvents within a certain range of dielectric constant, and (3) low fiber yield.[8,9]

However, with the advent of Forcespinning™ technology, the obstacles commonly encountered with use of electrospinning are overcome. Forcespinning uses centrifugal forces to promote fiber elongation; therefore, both conductive and nonconductive polymer solutions and polymer melts fiber can be spun without the need of electric fields.[6,10] Also the productivity of this method (1 g/min using a 1-prong spinneret), at the lab scale, has considerable gains over laboratory scale electrospinning (0.3 g/h).[9] The morphology of forcespun fibers is dependent on solution parameters and device configurations such as solution/melt viscosity, orifice diameter, and fiber collection methods.

Polycaprolactone (PCL) is a biocompatible and bioresorbable semicrystalline aliphatic polyester that has found uses in both industrial and biomedical applications.[11] The biodegradable nature of PCL can be attributed to the hydrolytic degradation of its ester bond and ultimately the nontoxic degradation metabolites that are formed and either secreted directly or metabolized in the Krebs cycle.[12–14] PCL as a homopolymer has a degradation time between 2 and 4 years; however, the degradation time of PCL can be greatly varied when copolymerized with other biodegradable polymers.[15] Because of its biodegradability and exceptional mechanical properties,[16] PCL fibers have found extensive uses as

Correspondence to: Z. McEachin (ztmceachin@broncs.utpa.edu).

Contract grant sponsor: National Science Foundation (DMR; PREM-The University of Texas Pan American/University of Minnesota); contract grant number: 0934157

scaffolds or substrates for tissue engineering, drug delivery systems (DDSs), and constituent materials in various nanocomposites.[7,17]

PCL has been used extensively as a scaffold for cell regeneration in a wide array of tissues. Choi et al. have successfully created a PCL/Collagen nanofibrous scaffold in order to facilitate muscle cell regeneration in large skeletal muscle defects. They showed that these nanofibrous meshes support cell adhesion and proliferation and when aligned can augment the formation of myotubes.[18] Similarly, PCL has also shown promising results as a synthetic bone scaffold. Porter et al. have studied PCL nanofibers as a replacement to the common bone graft material, autogenous cancellous bone. They found that the PCL nanofibers provided a biomimetic environment in which there was an increase in both a short- and long-term response of mesenchymal stem cells as well as a significant increase in the production of the noncollagenous extracellular matrix proteins, osteocalcin, and osteopontin.[19]

Akin to tissue engineering, PCL has been used in the research of novel DDSs. Zamani et al. successfully encapsulated the antibiotic drug metronidazole benzoate (MET) in electrospun PCL nanofibers.[20] They concluded that the antibiotic was indeed released via diffusion through the PCL fibers, referring to this as Fickian diffusion. They also found that the PCL fibers retained their flexibility and length leading to the conclusion that MET encapsulated PCL fibers would be an ideal DDS for periodontal diseases. Kim et al. also designed a DDS in which PCL and polyethylene oxide fibers were layered upon each other to form a drug reservoir mat. It was found that the rate of drug release was directly related to the thickness of the PCL fiber mesh layer. They also found that the protein used to test the DDS had not lost any biological activity, further demonstrating the viability of PCL as a possible drug delivery material.[21]

Saeed et al. used PCL in the formation of PCL/carbon nanotube composite fibers.[22] The carbon nanotubes were found to be well dispersed and oriented along the fiber axes. Castro et al. used PCL grafted nanotubes in developing a novel conductive polymer composite. This carbon nanotubes (CNT)/PCL conductive polymer composite showed promising results as a possible sensor for the identification of organic vapors.[23]

Given the vast potential and successful application of PCL nanofibers, it is imperative to develop and employ a method that can produce these nanofibers in greater yield. To the authors' knowledge, this article reports the first attempt to prepare PCL nanofibers using Forcespinning™ method. Therefore, the objective of this study was to determine the optimum processing configurations and microstructure analysis of PCL fiber produced via Forcespinning™ technology. The effects of this method on the crystallinity of the polymer are analyzed using differential scanning calorimetry (DSC) and X-ray diffraction (XRD).

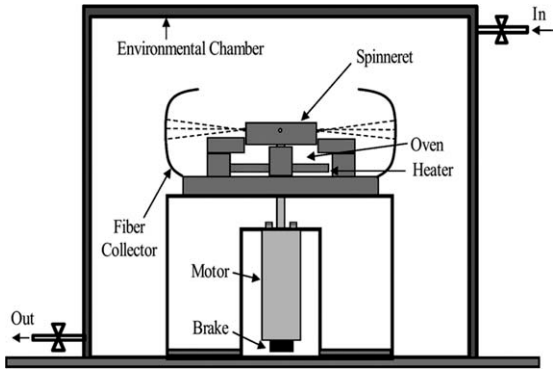

Figure 1 Schematic of Forcespinning™ setup.

EXPERIMENTAL

Materials

All polymers and solvents were purchased from Aldrich (Milwaukee, Wisconsin) and were used without further purification. PCL, with a number average molecular weight (M_n) of $\sim$ 60,000, was dissolved in dichloromethane in concentrations of 16 and 18 wt %. To prevent solvent loss during mixing, the polymer solutions were sealed in scintillation vials for $\sim$ 20 to 25 min and stirred using a magnetic stirrer.

Forcespinning™ setup

Figure 1 shows a schematic diagram of the Forcespinning™ apparatus setup. The spinneret was equipped with 30 gauge 1/2 inch regular bevel needles (Beckett-Dickerson). Using a 10-mL syringe, either 2 mL or 8 mL of the polymer solution was injected into the spinneret. The selection of solution volume is a result of the particular spinneret size chosen. The rotational speeds were varied from 3000 to 9000 rpm. At 3000 rpm, the solution was allowed to spin until depletion after $\sim$ 30 s, where at 9000 rpm, it took $\sim$ 10 s. A deep dish fiber collector with equally distanced vertical polytetrofluoroethylene pillars was used to collect fibers being elongated from the orifices of the spinneret. After collection, the fibers were covered and stored under desiccation.

Fiber analysis

The morphology of the collected PCL fibers (Fig. 2) was observed using scanning electron microscopy

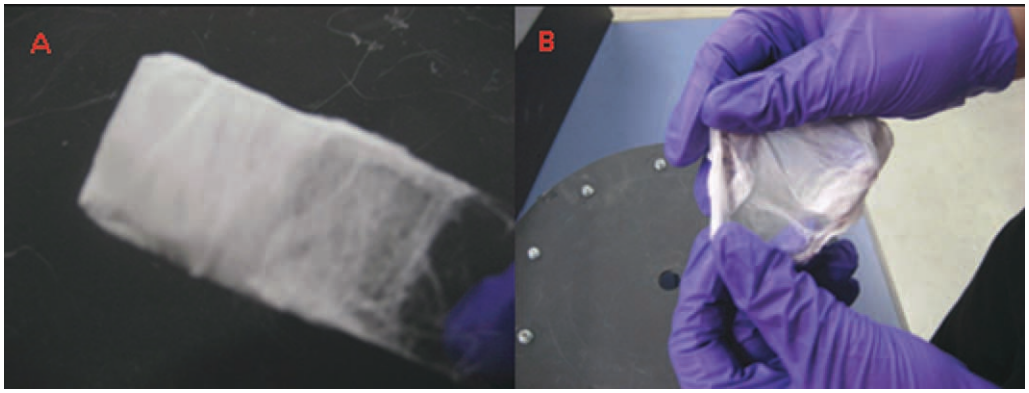

Figure 2 A: Fiber collection. B: PCL fiber mat. [Color figure can be viewed in the online issue, which is available at wileyonlinelibrary.com.]

(SEM, EVO LS10, Carl Zeiss, Germany). The samples were sputtered with gold-palladium before examination. X-ray diffraction of the PCL fibers and bulk PCL was performed with an X-ray diffractometer (AXS, Bruker). The XRD measurements were analyzed using Diffrac^{plus} EVA software (Bruker). DSC was performed on the PCL fibers and bulk PCL using a TA-Q series 500 DSC. Samples used for the DSC weighed $\sim$ 10 mg, and the scan was performed at a rate of 5°C/min between −80°C and 120°C. Percent crystallinity, χ_c, of the PCL samples was determined from the experimental heat of fusion ΔH_f, using 139.5 J/g as the heat of fusion for a 100% crystalline PCL sample.

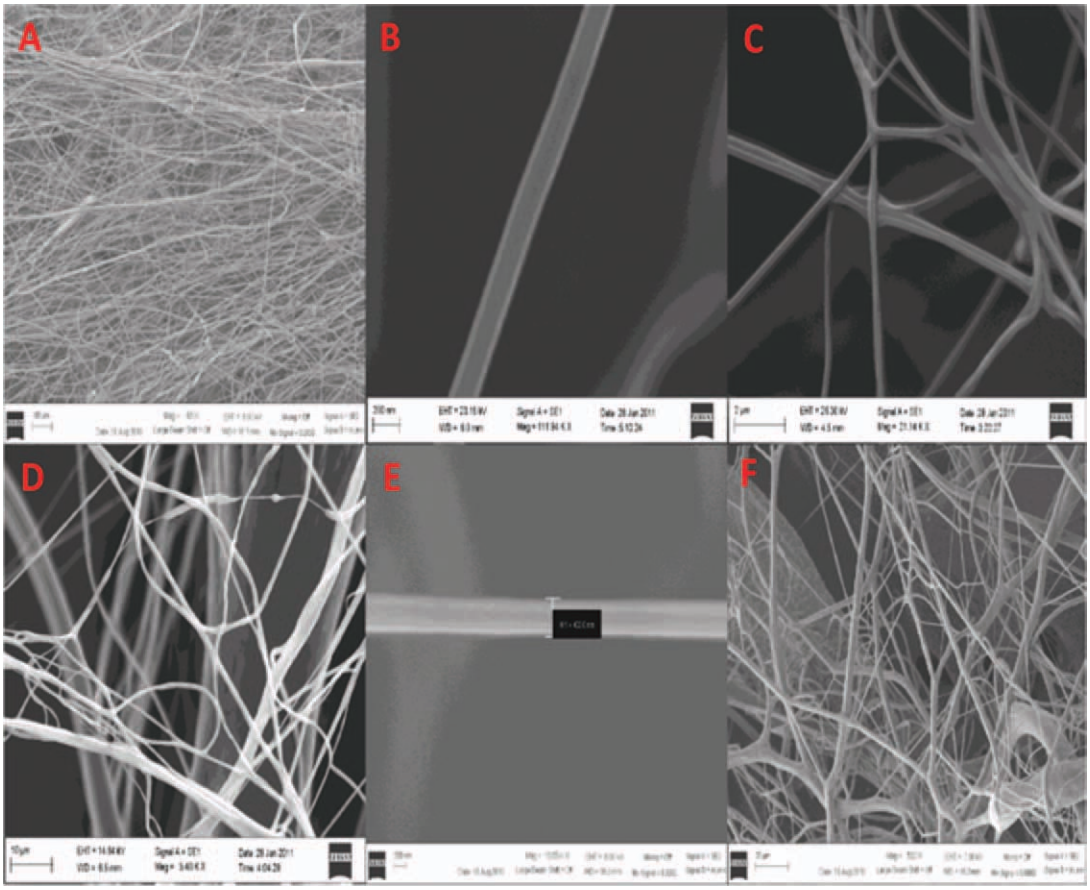

Figure 3 A: Fiber mesh 16% PCL-3000 rpm. B: Single PCL fiber 16% spun at 3000 rpm. C: 16% PCL fiber bundle spun at 3000 rpm. D: Bundle of 16% PCL fibers spun at 6000 rpm. E: Single 16% PCL fiber spun at 9000 rpm. F: 16% PCL fiber bundle spun at 9000 rpm. [Color figure can be viewed in the online issue, which is available at wileyonlinelibrary.com.]

TABLE I
Fiber Diameter of 16% PCL Fibers Spun at 3000, 6000, and 9000 rpm

Sample	Average diameter (nm)	Standard deviation (nm)
16%–3000	264	±125
16%–6000	326	±112
16%–9000	220	±98

RESULTS AND DISCUSSION

Characterization of PCL fibers

SEM micrographs of Forcespun fibers are shown in Figure 3. The fibers oriented in a random manner forming a three-dimensional mesh. Although both 16 wt % and 18 wt % solutions were tested, the 16 wt % solution was found to be optimal for sample preparation and handling. As can be seen in Table I, the average fiber size for the 16 wt % PCL fibers varied with spinneret speed. The smallest fiber average size was at 9000 rpm, though similar diameters were found at 3000 rpm. However, it should be noted that the fibers analyzed at 9000 rpm had a lower standard deviation when compared with fibers formed at 3000 rpm. Also, the speed at which fibers were formed affected the beading of the fibrous mats. The SEM micrographs in Figure 4 show an overview of the fibrous mats and the difference in beading between them. It can be observed that the degree of beading formation has an inverse relationship with rotational spinneret speed. The fibers spun at 3000 rpm had considerable beading, whereas at faster rotational speeds beading decreased with fibers spun at 9000 rpm having the least amount of beading.

In addition, a study on the relationship between fiber diameters of collected samples after various collection times was conducted. Fiber samples of 16% PCL spun at 6000 rpm were collected after three 5 s intervals. It was found that as the time increased the average fiber diameter of the samples decreased and the standard deviation of the collected samples narrowed (Table II). This indicates that after a critical time the average diameter of the collected fibers becomes more uniform (Fig. 5). This phenomenon is observed given that the fiber formation process is a combination of the imposed centrifugal force, the nozzle length and diameter, and the resultant aerodynamics forces that promote solvent evaporation and fiber elongation. In the first stage of the process, the polymer solution exits the nozzle in the form of a droplet that further elongates, given the viscoelastic properties of the material, slight swelling occurs at the tip of the nozzle which is overcame with time. If the system is stopped in the first stage, the fibers had not had time to overcome the elongation process nor has the solvent had time to evaporate. A complete theoretical and experimental study (including high-speed camera analysis) regarding fiber formation is currently under preparation.

DSC analysis

DSC data of both the bulk PCL and the 16 wt % PCL nanofibers forcespun at speeds 3000 rpm and 9000 rpm were obtained and tabulated in Table III. It is evident that the peak melting temperature (T_{mp}) of the nanofibers increased as well as the peak crystallization temperature (T_{cp}). However, the onset temperature of the melting endotherm (T_{op}) decreased. This lower onset temperature correlates with an extra peak apparent in the DSC melting endotherms of the fibers (Fig. 6). This decrease in onset temperature and the apparent second peak in the melting endotherm are attributed to the formation of an oriented mesophase resulting from incomplete crystallization due to rapid extensional flow. Figure 7 shows the endotherm peaks of the as-formed fibers and the second DSC cycle after deletion of thermal history. It can be seen that after erasing thermal history the original 16% fiber sample

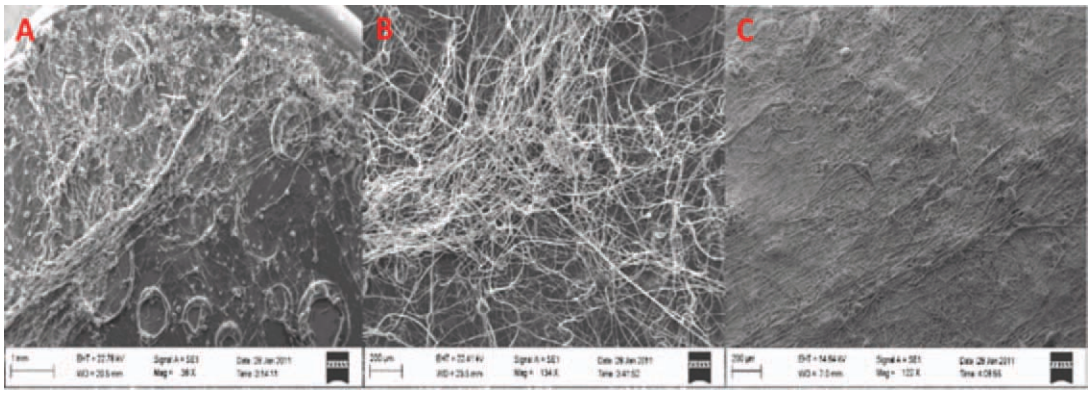

Figure 4 Effects of spinneret speed on beading of fiber mats. A: 3000 rpm. B: 6000 rpm. C: 9000 rpm. [Color figure can be viewed in the online issue, which is available at wileyonlinelibrary.com.]

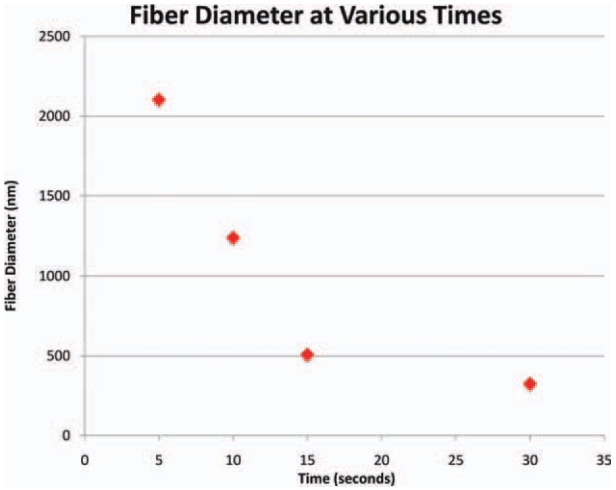

Figure 5 Graph of fiber diameter versus time for the 16% 6000 rpm PCL. [Color figure can be viewed in the online issue, which is available at wileyonlinelibrary.com.]

contains only one relatively sharp peak without the aligned mesophase. The crystallinity of each sample was calculated according to the equation:

$$\chi_c = \frac{\Delta H_m - \Delta H_c}{\Delta H_f}$$

where ΔH_m is the enthalpy of fusion, ΔH_c is the enthalpy of cold crystallization, and ΔH_f is the enthalpy of fusion of a 100% crystalline sample.

DSC data (Table III) shows that the degree of crystallinity of the forcespun fibers decrease relative to the bulk sample. Moreover, it can be observed that there is a decrease in the crystallinity of the 16% fibers with an increase in rotational speed.

As explained above, when fibers are rotated at higher speeds and longer times, the fiber diameter decreases, the polymer chains are further aligned given rise to the aligned mesophase with incomplete crystallization given fast elongation and solvent evaporation rate. Similar to electrospun fibers, the morphology and crystallinity of forcespun fibers seem to be highly dependent on both solvent evaporation rate and collector distance; thus, this decreased time frame of evaporation due to an increase in rotational speed ultimately restricts the extent to which crystallites are able to form in the collected fibers.

TABLE II
Average Fiber Diameter of 16% PCL 6000 rpm Collected After 5, 10, 15, and 30 sec

Sample	Average diameter (nm)	Standard deviation (nm)
16%–5	2105.2	±1004.3
16%–10	1238.7	±895.5
16%–15	508.7	±255.6
16%–30	326.0	±112.0

X-ray diffraction analysis

Figure 8 shows the X-ray diffraction spectra for the bulk and PCL nanofibers. The intensity of the bulk peak is higher than that of the various fiber peaks. Because crystallinity is a measure of the area of the peaks over the area of the whole, it can be determined that the production of PCL nanofibers lowered crystallinity, which is consistent with the collected DSC data. Two intense 2θ peaks were observed at $2\theta = 21.5^\circ$ and $2\theta = 23.9^\circ$, and these peaks coincide with previously observed 2θ peaks present in PCL fibers formed via electrospinning.[24]

CONCLUSIONS

Forcespinning™ technology was used to produce PCL nanofibers. The degree of beading as well as the diameter size of the individual fibers is dependent on spinneret speed. It was found that fibers spun at 9000 rpm produced nearly bead-less mats as well as fibers with average diameters of 220 nm. It was also found that the production of PCL fibers via Forcespinning™ technology induced a crystalline mesophase attributed to processing, which is not present in the bulk samples. It was observed that bulk PCL has a higher degree of crystallinity than PCL nanofibers and that fiber crystallinity was inversely proportional to rotational spinneret speeds. Forcespinning™ proves to be a successful method to fabricate long, continuous, and homogenous PCL nanofibers in high yield (at lease 1 g/min in the lab

TABLE III
Data Summary of Bulk PCL and 16% Forcespun Fibers at Different rpm

	Melting (T_m)			Crystallization (T_c)			% Crystallinity (X_c)
Sample	T_o	T_p	ΔH_m	T_o	T_p	ΔH_c	%
Bulk	51.5	55.81	110.5	30.40	22.58	78.00	23.2
16%–3000	42.66	58.76	122.9	36.76	33.76	97.35	18.3
16%–9000	43.36	59.61	120.0	34.90	28.84	95.85	17.3

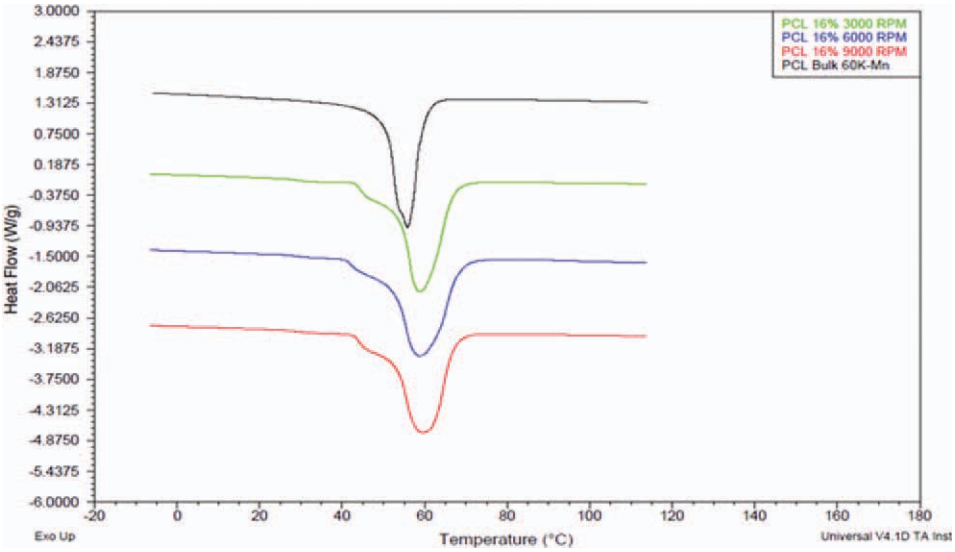

Figure 6 Melting endotherms of bulk PCL and 16% PCL forcespun fibers. [Color figure can be viewed in the online issue, which is available at wileyonlinelibrary.com.]

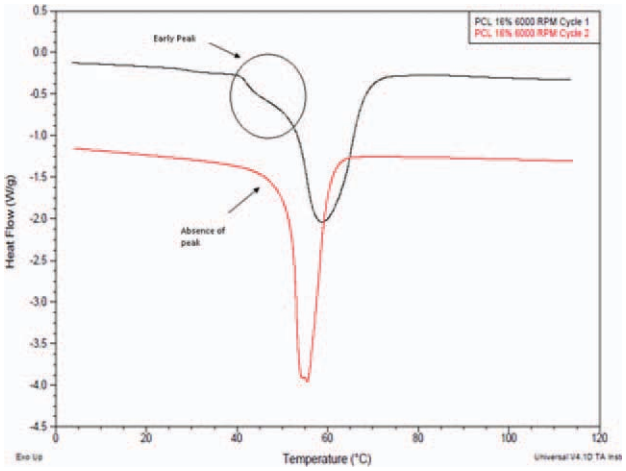

Figure 7 Melting endotherm of 16% PCL fiber showing absence of early peak after erasing of thermal history. [Color figure can be viewed in the online issue, which is available at wileyonlinelibrary.com.]

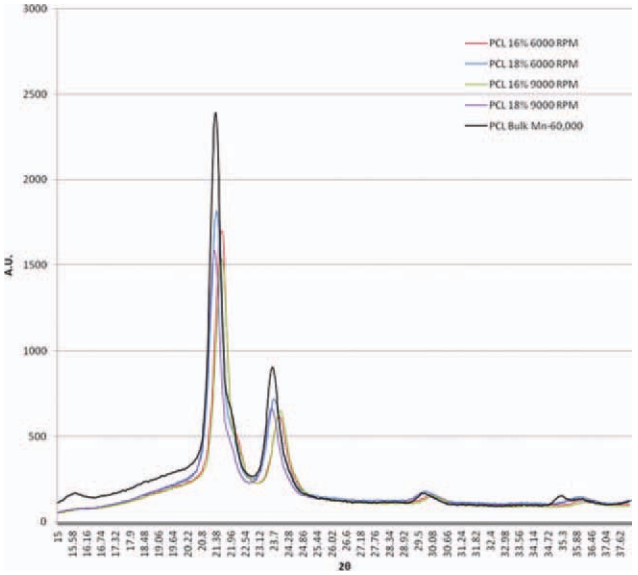

Figure 8 XRD spectra of 16% and 18% PCL fibers spun at 9000 rpm and 6000 rpm. [Color figure can be viewed in the online issue, which is available at wileyonlinelibrary.com.]

scale apparatus) where samples could be collected as nonwoven mats uniformly deposited on substrates or as free standing individual (continuous) fibers that can be aligned and spooled into yarns.

The authors thank Tom Eubanks and Sara Farhangi for assisting with SEM as well as Thomas Mion and Dr. Steven Tidrow for assisting with XRD.

References

1. Yoshimoto, H.; Shin, Y. M.; Terai, H.; Vacanti, J. P. Biomaterials 2002, 24, 2077.
2. Ito, Y.; Hasuda, H.; Kamitakahara, M.; Ohtsuki, C.; Tanihara, M.; Kang, I. K.; Kwon, O. H. J Biosci Bioeng 2005, 100, 43.
3. Grafe, T.; Graham, K. In Nonwovens in Filtration—5th International Conference; Stuttgart, Germany, March, 2003.
4. Karube, Y.; Kawakami, H. Polym Adv Technol 2009, 21, 861.
5. Li, D.; Xia, Y. Adv Mater 2004, 16, 1151.
6. Sarkar, K.; Lozano, K.; Zambrano, S.; Ramirez, M.; de Hoyos, E.; Vasquez, H. Mater Today 2010, 13, 42.
7. Paneva, D.; Bougard, F.; Manolova, N.; Dubois, P.; Rashkov, I. Eur Polym J 2008, 44, 566.
8. Baji, A.; Mai, Y.; Wong, S. C.; Abtahi, M.; Chen, P. Compos Sci Technol 2010, 70, 703.
9. Ramakrishna, S. An Introduction to Electrospinning and Nanofibers Technology; World Scientific Publishing Co.: Singapore, 2005; p 130.
10. Lozano, K.; Sarkar, K. U.S. Pat. 0,280,325, A1 (2009).

11. Lee, K. H.; Kim, H. Y.; Khil, M. S.; Ra, Y. M.; Lee, D. R. Polymer 2003, 44, 1287.
12. Cao, H.; Liu, T.; Chew, S. Y. Adv Drug Delivery Rev 2009, 61, 1055.
13. Nair, L. S.; Laurencin, C. T. Prog Polym Sci 2007, 32, 762.
14. Heath, D.; Christian, P.; Griffin, M. Biomaterials 2002, 23, 1519.
15. Woodruff, M. A.; Hutmacher, D. W. Prog Polym Sci 2010, 35, 1217.
16. Jeon, H. J.; Kim, J. S.; Kim, T. G.; Kim, J. H.; Yu, W. R.; Youk, J. H. Appl Surf Sci 2008, 254, 5886.
17. Nirmala, R.; Nam, K. T.; Park, D. K.; Woo-il, B.; Navamathavan, R.; Kim, H. Y. Surf Coat Technol 2010, 205, 174.
18. Choi, J. S.; Lee, S. J.; Christ, G.; Atala, A.; Yoo, J. Biomaterials 2008, 29, 2899.
19. Porter, J.; Henson, A.; Popat, K. Biomaterials 2009, 30, 780.
20. Zamani, M.; Morshed, M.; Varshosaz, J.; Jannesari, M. Eur J Pharm Biopharm 2010, 75, 179.
21. Kim, G. H.; Yoon, H.; Park, Y. K. Appl Phys A 2010, 100, 1197.
22. Saeed, K.; Park, S. Y.; Lee, H. J.; Baek, J. B.; Huh, W. S. Polymer 2006, 47, 8019.
23. Castro, M.; Lu, J.; Bruzaud, S.; Kumar, B.; Feller, J. F. Carbon 2009, 47, 1930.
24. Wong, S. C.; Baji, A.; Leng, S. Polymer 2008, 49, 4713.